Project 2 - TMA4212
Numerical Solution of Differential Equations by Difference Methods

Mari Norfolk
Lisa Marie F. Austad
Ola Rønnestad Abrahamsen

April 2024

1 Introduction

Our report investigates the stationary behavior of a substance undergoing convection and diffusion in a one-dimensional setting, focusing on its transport, mixing, and decay within a finite tube. We model this using a boundary value problem with a Poisson-like equation:

$$-\partial_x(\alpha(x)\partial_x u) + \partial_x(b(x)u) + c(x)u = f(x) \quad \text{in} \quad \Omega = (0,1), \tag{1}$$

where $u(x)$ represents concentration, $\alpha(x) > 0$ is the diffusion coefficient, $b(x)$ the convection velocity, $c(x)$ the decay rate, and $f(x)$ a source term. This model is grounded in conservation of mass, Fick's law, and Reynold's transport theorem.

2 Theory

Consider (1) and assume $\alpha(x) = \cos\left(\frac{\pi}{3}x\right)$, $c = 5$, $\|b\|_{L^\infty} + \|f\|_{L^2} < \infty$, and that we have Dirichlet boundary conditions $u(0) = 0 = u(1)$. For the theory part we denote $u(x) = u$, $v(x) = v$, $\alpha(x) = \alpha$, $\mathrm{b}(x) = \mathrm{b}$ and $\mathrm{c}(x) = \mathrm{c}$.

Claim: Any classical solution u of (1) satisfies $a(u,v) = F(v) \quad \forall v \in H_0^1(0,1)$, where $a(u,v) = \int_0^1 (\ldots - \mathrm{b}uv_x + cuv)\,\mathrm{d}x$.

Proof: Let $(-\mathcal{L}u)v = f(x)v$, for some $v \in H_0^1(0,1)$, then we can express the problem as

$$-\partial_x(\alpha\partial_x u)\,v + \partial_x(\mathrm{b}u)v + \mathrm{c}uv = f(x)v.$$

$$\implies \int_0^1 (-\partial_x(\alpha\partial_x u))\,v\mathrm{d}x + \int_0^1 (\partial_x(\mathrm{b}u))\,v\mathrm{d}x + \int_0^1 (\mathrm{c}u)v\mathrm{dx} = \int_0^1 f(x)v\mathrm{d}x$$

Further, we perform integration by parts to obtain:

$$\begin{aligned} &-(\alpha\partial_x u)v|_0^1 + \int_0^1 (\alpha\partial_x u)\partial_x v\,\mathrm{d}x + (\mathrm{b}u)v|_0^1 - \int_0^1 (\mathrm{b}u)\partial_x v\,\mathrm{d}x + \int_0^1 (\mathrm{c}u)v\,\mathrm{d}x \\ &\overset{v(0)=v(1)=0}{=} \int_0^1 (\alpha\partial_x u)\partial_x v\,\mathrm{d}x - \int_0^1 (\mathrm{b}u)\partial_x v\,\mathrm{d}x + \int_0^1 (\mathrm{c}u)v\,\mathrm{d}x = \int_0^1 f(x)v\,\mathrm{d}x. \end{aligned}$$

Then a and F is defined as

$$a(u,v) = \int_0^1 (\alpha\partial_x u)\partial_x v - (bu)\partial_x v + (cu)v\,\mathrm{d}x, \quad F(v) = \int_0^1 f(x)v\,\mathrm{d}x. \qquad \square$$

Claim (F1 and F2): The map $F : H^1 \to \mathbb{R}$, where $\mathbb{R}$ is equipped with the usual norm, is a bounded linear functional on H^1.

Proof: Consider the operator norm of F, denote $H^{1'}$ as the dual space of H^1 and we obtain

$$\|F\|_{H^{1'}} = \sup_{\substack{v\in H_0^1 \\ v\neq 0}} \frac{|F(v)|}{\|v\|_{H^1}} = \sup_{\substack{v\in H_0^1 \\ v\neq 0}} \frac{\left|\int_0^1 f(x)v(x)\,\mathrm{d}x\right|}{\|v\|_{H^1}}$$

Then by Cauchy-Schwarz inequality, this gives the final bound:

$$\|F\|_{H^{1'}} \leq \frac{\|f\|_{L^2}\|v\|_{L^2}}{\|v\|_{H^1}} \overset{\|v\|_{H^1}\geq\|v\|_{L^2}}{\leq} \|f\|_{L^2} < \infty,$$

using the assumption stated above that $\|f\|_{L^2} < \infty$.

To prove linearity, let $q \in \mathbb{R}$ and $u, v \in H^1$.

$$F(qv+u) = \int_0^1 f(x)(qv+u)\,\mathrm{d}x = \int_0^1 qf(x)v\,\mathrm{d}x + \int_0^1 f(x)u\,\mathrm{d}x = qF(v) + F(u). \qquad \square$$

Claim (A1): a is bilinear on $H^1 \times H^1$.

Proof: This can be proved through linearity of integration and differentiation. Assume $q \in \mathbb{R}$ and $u_1, u_2, v \in H^1$.

$$\begin{aligned}
a(qu_1 + u_2, v) &= \int_0^1 (\alpha\partial_x(qu_1 + u_2)\partial_x v - (b(qu_1 + u_2))\partial_x v + (c(qu_1 + u_2))v) \, \mathrm{d}x \\
&= q \int_0^1 (\alpha\partial_x u_1 \partial_x v - (bu_1)\partial_x v + (cu_1)v) \, \mathrm{d}x + \int_0^1 (\alpha\partial_x u_2 \partial_x v - (bu_2)\partial_x v + (cu_2)v) \, \mathrm{d}x \\
&= qa(u_1, v) + a(u_2, v).
\end{aligned}$$

One can perform a similar proof to prove the linearity in the second argument. □

Claim (A2): a is continuous on $H^1 \times H^1$. This means that $\exists\, C > 0$ s.t. $|a(u, v)| \le C\|u\|_V \|v\|_V \; \forall\, v, u \in V$, since boundedness implies continuity for bilinear forms.

Proof: Noting that $v, u \in H^1$,

$$\begin{aligned}
|a(u, v)| &= \left| \int_0^1 (\alpha\partial_x u)\partial_x v - (bu)\partial_x v + (cu)v \, \mathrm{d}x \right| \\
&\le |\langle \alpha\partial_x u, \partial_x v\rangle_{L^2(0,1)}| + |\langle bu, \partial_x v\rangle_{L^2(0,1)}| + |\langle cu, v\rangle_{L^2(0,1)}| \\
&\overset{C.S}{\le} \|\alpha\|_{L^\infty}\|\partial_x u\|_{L^2}\|\partial_x v\|_{L^2} + \|b\|_{L^\infty}\|u\|_{L^2}\|\partial_x v\|_{L^2} + \|c\|_{L^\infty}\|u\|_{L^2}\|v\|_{L^2} \\
&\overset{P.I}{\le} \|\alpha\|_{L^\infty}\|\partial_x u\|_{L^2}\|\partial_x v\|_{L^2} + 2\|b\|_{L^\infty}\|\partial_x u\|_{L^2}\|\partial_x v\|_{L^2} + \|c\|_{L^\infty}\|u\|_{L^2}\|v\|_{L^2} \\
&= (\|\alpha\|_{L^\infty} + 2\|b\|_{L^\infty})\|\partial_x u\|_{L^2}\|\partial_x v\|_{L^2} + \|c\|_{L^\infty}\|u\|_{L^2}\|v\|_{L^2} \\
&\le (\|\alpha\|_{L^\infty} + 2\|b\|_{L^\infty})\|u\|_{H^1}\|v\|_{H^1} + \|c\|_{L^\infty}\|u\|_{H^1}\|v\|_{H^1} \\
&= (\|\alpha\|_{L^\infty} + 2\|b\|_{L^\infty} + \|c\|_{L^\infty})\|u\|_{H^1}\|v\|_{H^1} = C\|u\|_{H^1}\|v\|_{H^1},
\end{aligned}$$

where we have used Cauchy-Schwarz and Poincarés inequality (our domain Ω is $(0, 1)$ and thus the constant in the inequality $\alpha_0 = 2$), as well as the fact that $\|u\|_{L^2} + \|\nabla u\|_{L^2} = \|u\|_{H^1}$ such that $\|u\|_{L^2}$, $\|\nabla u\|_{L^2} \le \|u\|_{H^1}$. □

Claim: Consider $a(u, u)$ where α, b, $c \in \mathbb{R} \setminus \{0\}$, then a satisfies the Gårding´s inequality which is given by

$$a(u, u) \ge \left(\alpha_0 - \frac{\varepsilon}{2}\|b\|_{L^\infty}\right) \int_0^1 u^2 \, \mathrm{d}x + \left(c_0 - \frac{1}{2\varepsilon}\|b\|_{L^\infty}\right) \int_0^1 u^2 \, \mathrm{d}x \quad \text{for all} \quad \varepsilon > 0,$$

where $\alpha_0 = \min_{x\in[0,1]} \alpha(x)$ and $c_0 = \min_{x\in[0,1]} c(x)$.

Proof:

$$\begin{aligned}
a(u, u) &\ge \alpha_0 \int_0^1 (\partial_x u)^2 \, \mathrm{d}x - \|b\|_{L^\infty} \int_0^1 u\partial_x u \, \mathrm{d}x + c_0 \int_0^1 u^2 \, \mathrm{d}x. \\
&\overset{Y.I}{\ge} \alpha_0 \int_0^1 u_x^2 \, \mathrm{d}x - \|b\|_{L^\infty} \left(\int_0^1 \frac{1}{2\varepsilon}u^2 + \frac{\varepsilon}{2}u_x^2 \, \mathrm{d}x \right) + c_0 \int_0^1 u^2 \, \mathrm{d}x. \\
&= (\alpha_0 - \frac{\varepsilon}{2}\|b\|_{L^\infty}) \int_0^1 u_x^2 \, \mathrm{d}x + (c_0 - \frac{1}{2\varepsilon}\|b\|_{L^\infty}) \int_0^1 u^2 \, \mathrm{d}x
\end{aligned}$$

where, Y.I is Youngs inequality. □

Claim (A3): a is coercive when $\|b\|_{L^\infty} < \sqrt{5}$, that is $\exists\, \gamma > 0$ s.t. $a(u, v) \ge \gamma\|u\|^2_{H^1} \; \forall\, v \in H^1$.

Proof: We can use the Gårding inequality to prove that a is coercive when $\|b\|_{L^\infty} < \sqrt{2\alpha_0 c_0} = \sqrt{5}$. This gives $c_0 > \frac{\|b\|^2_{L^\infty}}{2\alpha_0}$, and it follows that

$$a(u, u) \ge (\alpha_0 - \frac{\varepsilon}{2}\|b\|_{L^\infty}) \int_0^1 u_x^2 \, dx + \left(\frac{\|b\|^2_{L^\infty}}{2\alpha_0} - \frac{1}{2\varepsilon}\|b\|_{L^\infty} \right) \int_0^1 u^2 \, dx.$$

In order to be coercive we need the coefficient $\gamma > 0$, by using that the Gårding inequality is true for all $\varepsilon > 0$ we can chose ε such that both coefficients become positive.

$$\alpha - \frac{\epsilon}{2}\|b\|_{L^\infty} > 0 \quad \text{and} \quad \frac{\|b\|_{L^\infty}^2}{2\alpha} - \frac{1}{2\epsilon}\|b\|_{L^\infty} > 0 \Rightarrow \alpha - \frac{\epsilon}{2}\|b\|_{L^\infty} > 0 \Rightarrow \epsilon < \frac{2\alpha}{\|b\|_{L^\infty}}$$

$$\frac{\|b\|_{L^\infty}^2}{2\alpha} - \frac{1}{2\epsilon}\|b\|_{L^\infty} > 0 \Rightarrow \epsilon > \frac{\alpha}{\|b\|_{L^\infty}} \Rightarrow \frac{\alpha}{\|b\|_{L^\infty}} < \epsilon < \frac{2\alpha}{\|b\|_{L^\infty}}.$$

Thus, by choosing ε in this interval we obtain

$$a(u,u) \geq \left(\alpha - \frac{\varepsilon}{2}\|b\|_{L^\infty}\right)\|u_x\|_{L^2}^2 + \left(\frac{\|b\|_{L^\infty}^2}{2\alpha} - \frac{1}{2\varepsilon}\|b\|_{L^\infty}\right)\|u\|_{L^2}^2 \geq \gamma\|u\|_{H^1}^2$$

where γ is defined as the minimum of $\left\{\alpha - \frac{\varepsilon}{2}\|b\|_{L^\infty}, \frac{\|b\|_{L^\infty}^2}{2\alpha} - \frac{1}{2\varepsilon}\|b\|_{L^\infty}\right\}$. $\square$

Thus, A1, A2 and A3 is satisfied as well as F1 and F2. Then by the Lax-Milgram theorem this implies the existence of a unique solution $u \in H_0^1(0,1)$ for $a(u,v) = F(v)$ for all $v \in H_0^1(0,1)$.

Claim (Galerkin Orthogonality): Let u and u_h be solutions to the infinite and finite dimensional variational problems, respectively. Then $a(u - u_h, v_h) = 0 \quad \forall v_h \in V_h$, where $V_h = X_h^1(0,1) \cap H_0^1(0,1)$ is the space of continuous functions with zero boundary values, that are piecewise linear on the "triangulation" given by the grid.

Proof: For any arbitrary $v_h \in V_h$ and by using that a is bilinear:

$$a(u - u_h, v_h) = a(u, v_h) - a(u_h, v_h) = F(v_h) - F(v_h) = 0. \quad \square$$

Claim (Cea's Lemma): Under the assumption that (A1)-(A3) holds, and $u \in V$, $v_h \in V_h$ solve (V) and (V_p),

$$\|u - u_h\|_{H^1} \leq \frac{C}{\gamma}\inf_{v_h \in V_h}\|u - v_h\|_{H^1}, \quad \forall v_h \in V_h.$$

Proof: Due to (A3), coercivity, we obtain

$$\|u - u_h\|_{H^1}^2 \leq \frac{1}{\gamma}a(u - u_h, u - u_h).$$

Thus we can expanding the right-hand side to get,

$$a(u - u_h, u - u_h) = a(u - u_h, u - u_h + v_h - v_h) = a(u - u_h, u - v_h) + \underbrace{a(u - u_h, v_h - u_h)}_{=0},$$

due to Galerkin orthogonality, as $v_h - u_h \in V_h$. Thus, by using (A2) we obtain,

$$\|u - u_h\|_{H^1}^2 \leq \frac{1}{\gamma}a(u - u_h, u - v_h) \leq \frac{C}{\gamma}\|u - u_h\|_{H^1}\|u - v_h\|_{H^1}.$$

Since this holds for all $v_h \in V_h$ the inequality also holds for the infimum and dividing by $\|u - u_h\|_{H^1}$ on both sides we obtain:

$$\|u - u_h\|_{H^1} \leq \frac{C}{\gamma}\inf_{v_h \in V_h}\|u - v_h\|_{H^1}. \quad \square$$

Claim: The error related to the H^1-norm is bounded.

Proof: Firstly we claim without proof that for $u \in H^2$, $\inf_{v_h \in X_h^1}\|u - v_h\|_{H^1} \leq Ch\|u_{xx}\|_{L^2}$. Thus, we can use Cea´s lemma to derive the error bound. Further we choose $v_h = I_h u = \sum_{i=0}^{M} u(x_i)\varphi_i(x)$, where $I_h u$ is the interpolation of u in the finite state space V_h and $\varphi_i(x)$ is the hat function and make up the basis for V_h. Especially note that $I_h u \in X_h^1 \cap H_0^1(0,1)$. Then one can show:

$$\|u-u_h\|_{H_1} \overset{Cea}{\leq} \frac{C}{\gamma}\|u-v_h\|_{H^1} = \frac{C}{\gamma}\|u-I_h u\|_{H^1} \leq \frac{C'}{\gamma} h \|u_{xx}\|_{L^2}. \quad \square$$

Claim: We additionally state, without proof, that for functions in H^2, using the L^2-norm one achieves quadratic convergence for the error bound.

Further we define on $[0,1]$ the functions:

$$w_1(x) = \begin{cases} \frac{x}{\frac{\sqrt{2}}{2}}, & x \in \left[0, \frac{\sqrt{2}}{2}\right] \\ \frac{1-x}{1-\frac{\sqrt{2}}{2}}, & x \in \left(\frac{\sqrt{2}}{2}, 1\right], \end{cases} \qquad \text{and} \qquad w_2(x) = x - x^{\frac{3}{4}}$$

Definition (Weak derivative): Let $u \in L^2((0,1))$. We say that $u'(x)$ is a weak derivative of u if, for all smooth functions v such that $v(0) = v(1) = 0$, we have

$$\int_0^1 u'(x)v(x)\,dx = -\int_0^1 u(x)v'(x)\,dx$$

Claim: Both functions w_1 and w_2 belong to $H^1(0,1)$, but not to $H^2(0,1)$

Proof: Recall that the spaces H^k are defined as k-times weakly-differentiable functions with L^2 weak derivatives.

First, note that $w_1, w_2 \in L^2$. Further, we define the smooth function

$$\phi(x) = x(1-x), \text{ s.t. } \phi(0) = 0 = \phi(1)$$

With this, we claim that $w_2' = 1 - \frac{3}{4}x^{-\frac{1}{4}}$ is a weak derivative of w_2.

$$\int_0^1 w_2' x(1-x)\,dx = \int_0^1 (1-\frac{3}{4}x^{-\frac{1}{4}})x(1-x)\,\mathrm{d}x = \frac{5}{462} = -\int_0^1 (x - x^{\frac{3}{4}})(1-2x)\,\mathrm{d}x = -\int_0^1 w_2(1-2x)\,\mathrm{d}x$$

Thus, we have proven that w_2 has a weak derivative and that it is $w_2' = 1 - \frac{3}{4}x^{-\frac{1}{4}}$.

Further, it can be shown by integration that also $w_2' \in L^2$ and thus $w_2 \in H^1(0,1)$. However, w_2' has weak derivative $w_2'' = \frac{3}{16}x^{-\frac{5}{4}}$, which can be shown to not be an element of L^2 by integration, and thus $w_2 \notin H^2(0,1)$.

Further, it can be shown that w_1 has the weak derivative

$$w_1'(x) = \begin{cases} \sqrt{2}, & x \in \left[0, \frac{\sqrt{2}}{2}\right) \\ -2-\sqrt{2}, & x \in \left(\frac{\sqrt{2}}{2}, 1\right], \end{cases} = \sqrt{2} - 2(1+\sqrt{2})H(x - \frac{\sqrt{2}}{2})$$

where H is the Heaviside step function. Thus, $w_1' \in L^2$, but $w_1'' \notin L^2$ as the weak derivative of Heaviside step function is the Dirac delta function, which is not an element of L^2. Thus $w_1 \in H^1(0,1)$ and $w_1 \notin H^2(0,1)$. $\square$

Claim: Given $f_1(x) = x^{-\frac{2}{5}}$ and $f_2(x) = x^{-\frac{7}{5}}$, $f_1 \in L^2(0,1)$ and $f_2 \notin L^2(0,1)$ for $x \in (0,1)$, that is, f_1 is square-integrable on the given interval and f_2 is not.

Proof: We want to prove that f_1 is square-integrable on the given interval and f_2 is not. Note that for the given interval both $f_2, f_1 > 0$, and thus $|f_1|^2 = f_1^2$, $|f_2|^2 = f_2^2$. It can be shown that for both these functions, their weak derivatives is also the strong derivatives. Further, this results in

$$\int_0^1 |f_1|^2 \mathrm{d}x = \int_0^1 f_1^2 \mathrm{d}x = \left[5x^{\frac{1}{5}}\right]_0^1 < \infty$$

$$\int_0^1 |f_2|^2 \mathrm{d}x = \int_0^1 f_2^2 \mathrm{d}x = \left[-\frac{5}{9}x^{-\frac{9}{5}}\right]_0^1 = \infty$$

Thus, $f_1 \in L^2(0,1)$ and $f_2 \notin L^2(0,1)$. $\square$

3 Numerical methods and tests

First, let $\alpha > 0, b, c > 0$ be nonzero constants. After specifying a triangularization of the domain of the equation and expanding in terms of the basis, solving the (weak) PDE is reduced to solving the linear system $Au = b$. Using the weak formulation one can define the 'stiffness matrix' A[1] and 'load vector' F by,

$$A_{ij} = \int_0^1 \varphi_i'(x)\varphi_j'(x)\mathrm{d}x = \sum_k \int_{x_k}^{x_{k+1}} \varphi_i'(x)\varphi_j'(x)\mathrm{d}x, \quad F_j = \int_0^1 f(x)\varphi_j(x)\mathrm{d}x = \sum_k \int_{x_k}^{x_{k+1}} f(x)\varphi_j(x)\mathrm{d}x.$$

where φ_j is the hat function. Thus, our numerical solution is mainly related to constructing A and F. In doing this it is important to note that each φ_i is only non-zero in the interval $(i-1, i+1)$, which simplifies the contributions to A and F significantly. By integration it can be shown that the entries in A is given by:

$$A_{i,i-1} = -\frac{\alpha}{h_i} - \frac{b}{2} + c\frac{h_i}{6}, \quad A_{i,i} = \frac{\alpha}{h_i} + \frac{\alpha}{h_{i+1}} + c\frac{h_i + h_{i+1}}{3}, \quad A_{i,i+1} = -\frac{\alpha}{h_{i+1}} + \frac{b}{2} + c\frac{h_{i+1}}{6}.$$

To construct F we use Simpson's method to approximate the integral given above.

3.1 Constructing F for non-smooth test solutions

However, when constructing F for non-smooth solutions this needs some refinement. The problem arises with the non existence of the second derivative. However, this can be solved using integration by parts. Consider the part of the integral concerning the second derivative and for ease ignore $-\alpha$ up front of the integral.

$$\begin{aligned}
&\int_0^1 \partial_x^2 w(x)\phi_i(x)\mathrm{d}x = \int_{x_{i-1}}^{x_i} \partial_x^2 w(x)\phi_i(x)\mathrm{d}x + \int_{x_i}^{x_{i+1}} \partial_x^2 w(x)\phi_i(x)\mathrm{d}x \\
&= \overbrace{[\phi_i(x)\partial_x w(x)]_{x_{i-1}}^{x_i}}^{\partial_x w(x_i)} - \int_{x_{i-1}}^{x_i} \partial_x w(x)\partial_x\phi_i(x)\mathrm{d}x + \overbrace{[\phi_i(x)\partial_x w(x)]_{x_i}^{x_{i+1}}}^{-\partial_x w(x_i)} - \int_{x_i}^{x_{i+1}} \partial_x w(x)\partial_x\phi_i(x)\mathrm{d}x \\
&= -\frac{1}{h_i}\int_{x_{i-1}}^{x_i} \partial_x w(x)\mathrm{d}x + \frac{1}{h_{i+1}}\int_{x_i}^{x_{i+1}} \partial_x w(x)\mathrm{d}x = -w\left(x_i\right)\left(\frac{1}{h_i} + \frac{1}{h_{i+1}}\right) + \frac{w\left(x_{i-1}\right)}{h_i} + \frac{w\left(x_{i+1}\right)}{h_{i+1}}.
\end{aligned}$$

This approach was used to solve for w_1 and w_2 in the part of the integral where one gets a second derivative, the other parts are again solved using quadrature.

3.2 Solving for u given $f(x)$

Now we want to solve for u given $f(x)$ and we use f_1 and f_2 defined in the theory. As proved earlier, $f_1 \in L^2(0,1)$ and we can compute the right-hand side in the same way as done above. However, $f_2 \notin L^2(0,1)$ and thus, it can be shown through integration by parts that for f_2 we get the following right-hand side by using that $f_2 = -\frac{5}{2}(f_1)_x$

$$F_j = \frac{5}{2}\int_0^1 f_1\varphi_j'\mathrm{d}x.$$

3.2.1 Refining the grid near singularity $(x = 0)$

In an attempt to improve the solution we want to refine the grid near the singularity through the use of a graded grid where $x_0 = 0$ and $x_i = r^{M-i}$, $i = 1, \dots, M$, for some $r \in (0,1)$. This amounts to putting more nodes near the singularity $x = 0$ of the right-hand side. In order to compute the error we use a reference solution computed on a very refined grid, and then we compare the errors from the graded and a uniform grid.

[1] An example of a stiffness matrix is provided in Appendix A

3.3 Verification of numerical solver

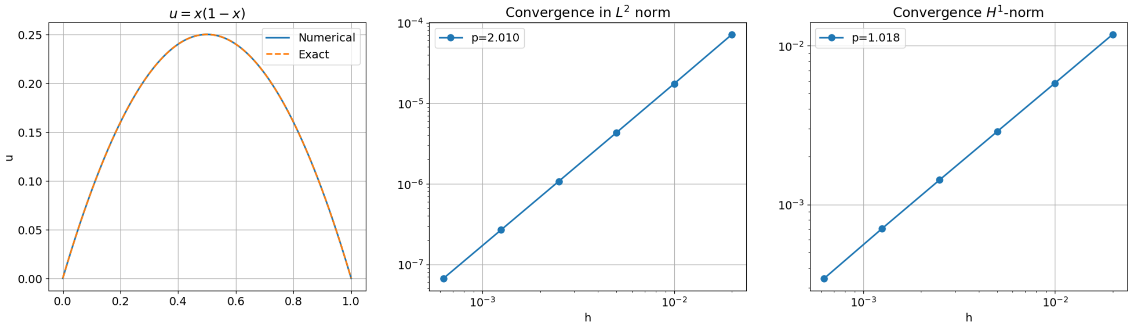

Figure 1: Numerical solution and convergence in L^2 and H^1 for $u(x) = x - x^2$ using $\alpha = b = c = 1$.

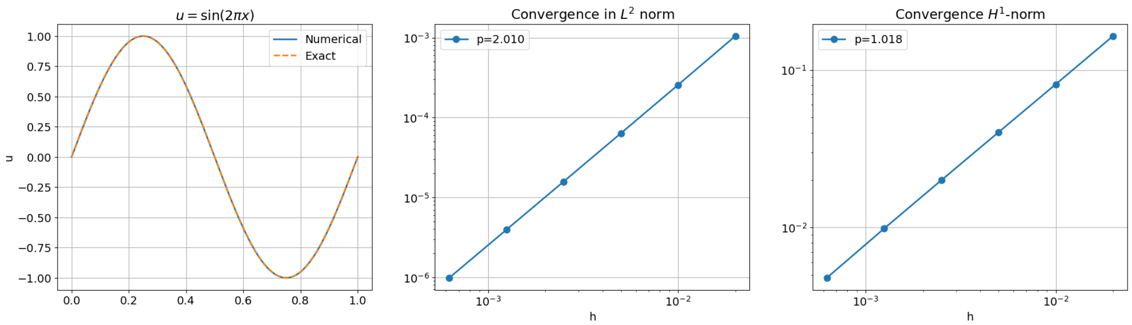

Figure 2: Numerical solution and convergence in L^2 and H^1 for $u(x) = \sin(2\pi x)$ using $\alpha = b = c = 1$.

The plots demonstrate a match between the numerical and exact solutions, reinforcing the reliability of our solver. Furthermore, the convergence plots reveal approximately linear convergence in the H^1 norm and quadratic convergence in the L^2 norm, aligning closely with theoretical expectations.

4 Results and discussion

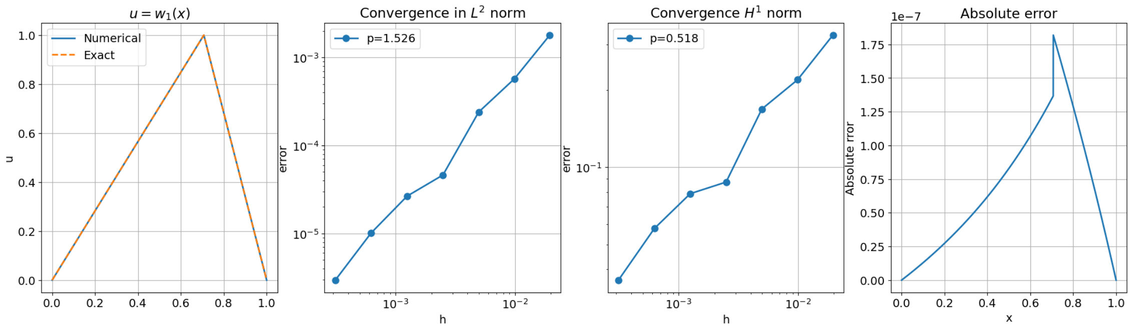

Figure 3: Numerical solution, convergence in L^2 and H^1 and absolute error for w_1 as defined earlier with $\alpha = b = c = 1$. Absolute error plot and solution plot produced with 3201 nodes.

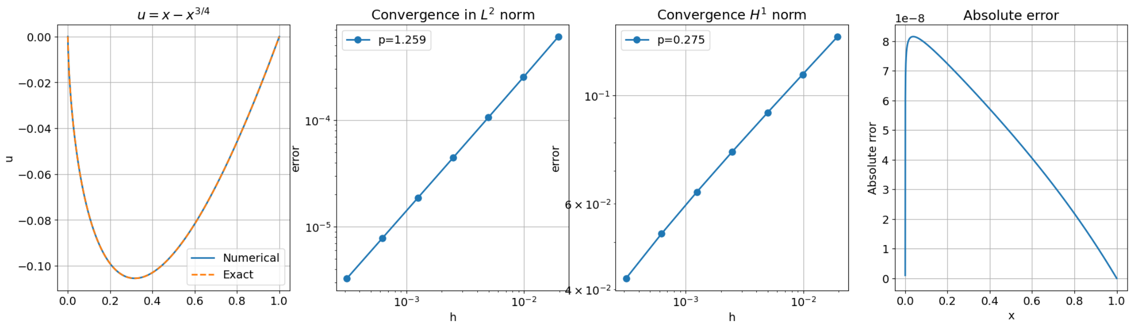

Figure 4: Numerical solution, convergence in L^2 and H^1 and absolute error for $w_2 = x - x^{\frac{3}{4}}$ using $\alpha = b = c = 1$. Absolute error plot and solution plot produced with 3201 nodes.

Testing with non-smooth functions one can observe that the convergence rates have declined for both norms. This can be grounded in the fact that $w_1, w_2 \notin H^2$ and that both error bounds assumes this inclusion.

The error plots also showcase clearly that the largest error for both functions are near the singularity, which motivates the next results, where we have refined the grid near the singularity in $x = 0$ in an attempt to reduce this error.

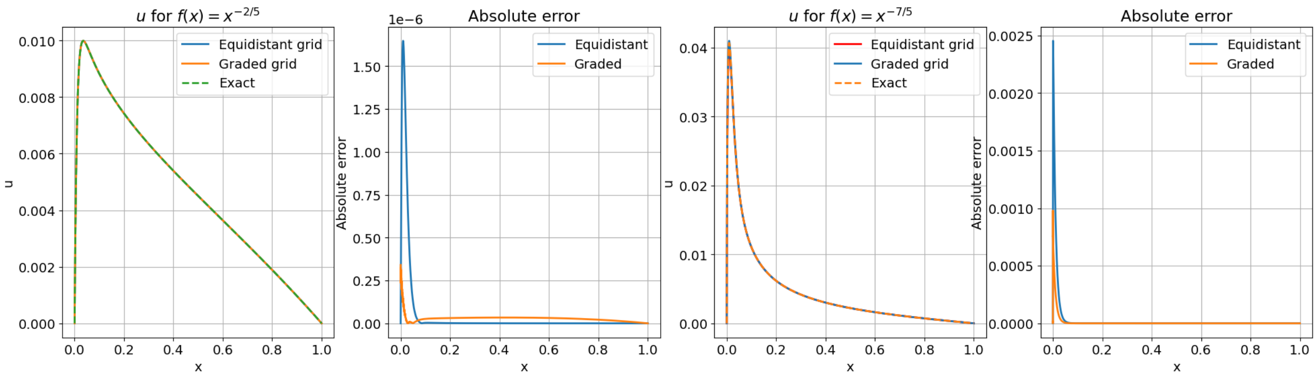

Figure 5: Numerical solution and absolute error for $f_1 = x^{-\frac{2}{5}}$ and $f_2 = x^{-\frac{7}{5}}$ for uniform and graded grid. Plots generated with $M = 1500, r = 0.99$ nodes, $\alpha = 1$, $b = -100$, $c = 100$.

When solving the problem with f_1 we observe a better result on the graded grid compared to the equidistant grid near the singularity, and slightly larger absolute error for the rest of the function. For f_2 the graded grid yields a smaller absolute error around the singularity. These results make sense as we would expect a better solution around singular points when we increase the number of nodes in these areas.

Table 1: Error Comparison for Different Nodes for f_2 with $r = 0.99, \alpha = 1, b = -100, c = 100$.

Nodes	L^2 Equi	L^2 Graded	H^1 Equi	H^1 Graded
200	9.140×10^{-4}	6.581×10^{-3}	5.178×10^{-1}	7.503×10^{-1}
400	5.494×10^{-4}	2.474×10^{-3}	4.251×10^{-1}	6.856×10^{-1}
800	3.296×10^{-4}	1.003×10^{-4}	3.362×10^{-1}	1.626×10^{-1}
1600	1.915×10^{-4}	6.488×10^{-5}	2.485×10^{-1}	7.630×10^{-2}
3200	1.025×10^{-4}	6.620×10^{-5}	1.537×10^{-1}	7.782×10^{-2}

From Table 1, we observe that the error in the L^2- and H^1-norm for the graded grid is smaller than for the equidistant for higher number of nodes when we use $r = 0.99$. For this choice of r, this is expected as for lower number of nodes we will not necessarily get more nodes around the singularity in the graded grid compared to the equidistant. For higher number of nodes we will have more nodes around the singularity resulting in a smaller error. The preferred number of nodes will be dependent on the value of r to get the smallest error. Further, the L^2-norm is clearly smaller then the H^1-norm which is what we expect from the definition of the norms. We have decided to exclude the error comparison table for f_1[2], as it does not offer much additional insights.

Given our findings, we believe that with a reasonable choice of r given the chosen number of nodes, the graded grid will be preferable on solutions with sharper gradients for all number of nodes.

5 Conclusion

In conclusion, our study on the stationary convection-diffusion problem within a one-dimensional framework has effectively demonstrated the capability of the finite element method in solving boundary value problems. Our approach confirmed the solver's accuracy and theoretical convergence rates. We also studied the significance of refining the grid near singularities.

[2]The error comparison table for f_1 is provided in Appendix A.

A Appendix

```
[[15.3        -5.4         0.          0.          0.        ]
 [-4.4         8.83333333 -3.68333333  0.          0.        ]
 [ 0.         -2.68333333  8.83333333 -5.4         0.        ]
 [ 0.          0.         -4.4        12.01666667 -7.09166667]
 [ 0.          0.          0.         -6.09166667 26.86666667]]
```

Figure 6: Example of a stiffness matrix with $\alpha = 1, b = -1, c = 3$ and nodes $[0, 0.1, 0.3, 0.6, 0.8, 0.95, 1]$.

Table 2: Error Comparison for Different Nodes for f_1 with $r = 0.99$

Nodes	L^2 Equi	L^2 Graded	H^1 Equi	H^1 Graded
200	1.586×10^{-5}	2.485×10^{-2}	1.254×10^{-2}	2.777×10^{-1}
400	4.026×10^{-6}	2.235×10^{-3}	6.105×10^{-3}	1.061×10^{-1}
800	1.016×10^{-6}	2.762×10^{-5}	2.800×10^{-3}	2.720×10^{-3}
1600	2.549×10^{-7}	3.427×10^{-8}	1.145×10^{-3}	2.664×10^{-5}
3200	6.270×10^{-8}	3.282×10^{-8}	3.126×10^{-4}	2.663×10^{-5}